Molecular Biology of the Cell
Vol. 7, 961–974, June 1996

Analysis of the Role of p200-containing Vesicles in Post-Golgi Traffic

Elina Ikonen, Robert G. Parton,† Frank Lafont, and Kai Simons*

Cell Biology Programme, European Molecular Biology Laboratory, Postfach 10.2209, D-69012 Heidelberg, Germany

Submitted December 22, 1995; Accepted March 14, 1996
Monitoring Editor: Suzanne R. Pfeffer

p200 is a cytoplasmic protein that associates with vesicles budding from the trans-Golgi network (TGN). The protein was identified by a monoclonal antibody AD7. We have used this antibody to analyze whether p200 functions in exocytic transport from the TGN to the apical or basolateral plasma membrane in Madin-Darby canine kidney cells. We found that transport of the viral marker proteins, influenza hemagglutinin (HA) to the apical surface or vesicular stomatitis virus glycoprotein (VSV G) to the basolateral surface in streptolysin O-permeabilized cells was not affected when p200 was depleted from both the membranes and the cytosol. When vesicles isolated from perforated cells were analyzed by equilibrium density gradient centrifugation, the p200 immunoreactive membranes did not comigrate with either the apical vesicle marker HA or the basolateral vesicle marker VSV G. Immunoelectron microscopy of perforated and double-labeled cells showed that the p200 positive vesicular profiles were not labeled by antibodies to HA or VSV G when the viral proteins were accumulated in the TGN. Furthermore, the p200-decorated vesicles were more electron dense than those labeled with the viral antibodies. Together, these results suggest that p200 does not function in the transport pathways that carry HA from the TGN to the apical surface or VSV G from the TGN to the basolateral surface.

INTRODUCTION

Intracellular traffic between the membrane-bound compartments of eukaryotic cells is mediated by vesicular carriers (Jamieson and Palade, 1967; Palade, 1975). A general mechanism for production of these transport intermediates is thought to involve the assembly of cytosolic proteins on the donor membrane at the site of the forming vesicle. This coated bud then pinches off to become a coated transport vesicle that releases its coat before fusion with the acceptor membrane. The first of these cytosolic coat proteins to be identified were clathrin and adaptors that coat endocytic vesicles budding from the plasma membrane and vesicles trafficking between the trans-Golgi network (TGN)[1] and endosomes (Pearse and Robinson, 1990). In the early secretory pathway, transport is mediated by vesicles coated with the COPI and COPII coat protein complexes (Rothman and Orci, 1992; Rothman, 1994; Barlowe *et al.*, 1994; Letourneur *et al.*, 1994). Recently, COPI-related proteins have been described in the endocytic pathway (Whitney *et al.*, 1995). However, in the late secretory routes, between the TGN and the plasma membrane, no coat proteins have so far been identified.

We have previously analyzed the composition of TGN-derived vesicles in Madin-Darby canine kidney (MDCK) epithelial cells (Bennett *et al.*, 1988; Wandinger-Ness *et al.*, 1990). In these cells, two distinct vesicle populations are formed in the TGN

* Corresponding author.
† Present address: Centre for Microscopy and Microanalysis and Department of Physiology and Pharmacology, University of Queensland, Queensland 4072, Brisbane, Australia.

[1] Abbreviations used: BFA, brefeldin A; BHK, baby hamster kidney; GMP-PNP, guanylyl-imidodiphosphate; HA, hemagglutinin; MDCK, Madin-Darby canine kidney; PBS, phosphate-buffered saline; SLO, streptolysin O; TGN, trans-Golgi network; VSV G, vesicular stomatitis virus glycoprotein.

to transport proteins and lipids selectively to either the apical or the basolateral plasma membrane domain. The realization that certain viral membrane glycoproteins are differentially sorted into the two routes (Rodriguez-Boulan and Pendergast, 1980) enabled the immunoisolation of apical and basolateral vesicles using antibodies against viral marker proteins (Wandinger-Ness *et al.*, 1990). This led to the characterization of their protein composition and identification of several vesicular membrane proteins (Kurzchalia *et al.*, 1992; Fiedler *et al.*, 1994, 1995; Zacchetti *et al.*, 1995). When the immunoisolated apical and basolateral vesicles were viewed by electron microscopy no obvious coat structure was observed (Wandinger-Ness *et al.*, 1990). However, a coat complex could have dissociated from the membrane during vesicle purification or it could have been difficult to visualize with the technique used.

Recently, in a panel of antibodies raised against canine liver Golgi membranes, a monoclonal antibody recognizing a 200-kDa protein was identified (Narula *et al.*, 1992). This p200 is a cytoplasmic phosphoprotein found in a wide variety of cell types, which associates preferentially with vesicles budding from the TGN in NRK cells (Narula and Stow, 1995). It has been proposed that the lace-like vesicle coat detected in the TGN contains the p200 protein (Ladinsky *et al.*, 1994). We therefore decided to test whether p200 could be involved in the formation of either apical or basolateral vesicles in MDCK cells. We analyzed the role of p200 as follows: 1) functionally by testing the effect of p200 depletion in apical and basolateral transport; 2) biochemically by comparing the sedimentation of p200-containing vesicles to that of apical and basolateral vesicles; and 3) morphologically by double-labeling of p200 and apical or basolateral marker proteins and observation by electron microscopy.

MATERIALS AND METHODS

Materials

Unless otherwise indicated, reagents were obtained from the sources described previously (Bennett *et al.*, 1988; Wandinger-Ness *et al.*, 1990; Pimplikar *et al.*, 1994). Guanylyl-imidodiphosphate (GMP-PNP) was obtained from Boehringer Mannheim (Mannheim, Germany) and brefeldin A (BFA) was obtained from Sigma (Deisenhofen, Germany). The hybridoma cells producing anti-p200 monoclonal antibody AD7 (Narula *et al.*, 1992) were provided by K. Matlin (Harvard Medical School, Boston, MA). The monoclonal antibodies directed against the cytoplasmic domains of vesicular stomatitis virus glycoprotein (VSV G) and PR8 HA were prepared as described by Kreis (1986) and Hughson *et al.* (1988), respectively. The polyclonal anti-Rab 6 antibody was provided by B. Goud (Institut Curie, Paris, France) and the polyclonal anti-VSV G antibody was provided by T. Nilsson (European Molecular Biology Laboratory, Heidelberg, Germany).

Cell Culture and Viral Infections

BHK (baby hamster kidney) and MDCK strain II cells were grown as previously described (Kurzchalia *et al.*, 1992; Pimplikar *et al.*, 1994). MDCK cells were seeded on 1.2-cm diameter filters according to the method of Ikonen *et al.* (1995) and on other filters according to the method of Wandinger-Ness *et al.* (1990). The viral strains and infection procedures have been described (Wandinger-Ness *et al.*, 1990; Pimplikar *et al.*, 1994).

Immunofluorescence Microscopy

Cells on glass coverslips were treated for 5 min with 5 μg/ml BFA or 30 min with AlF_4^- (50 μM $NH_4Al(SO_4)_2$ and 10 mM KF) in growth medium. The cells were fixed with 4% paraformaldehyde in phosphate-buffered saline (PBS) for 20 min, and the aldehyde groups quenched with 50 mM NH_4Cl in PBS. The cells were permeabilized with 0.1% Triton X-100 for 4 min, and unspecific antibody binding was blocked by incubating the cells in 10% heat-inactivated fetal calf serum for 30 min. The cells were incubated with undiluted AD7 hybridoma culture supernatant for 1 h at room temperature, washed with PBS, and the primary antibody visualized with tetramethyl rhodamine isothiocyanate-conjugated secondary antibody. The coverslips were viewed and photographed with an Axiophot photomicroscope (Carl Zeiss, Oberkochen, Germany). To test for depletion of p200 from permeabilized MDCK cells, cells were cultured on 1.2-cm diameter filters, permeabilized with streptolysin O (SLO), and cytosol depleted apically or basolaterally exactly as for the transport assays, except that for some filters 100 μM GMP-PNP was added to the depletion buffer. Immediately after cytosol depletion the cells were fixed in 4% paraformaldehyde and stained with AD7, incubating the primary antibody overnight at 4°C. To visualize sialyltransferase staining, human sialyltransferase cDNA tagged with the VSV G-epitope in pSRα vector (DNAX, Palo Alto, CA) (Rabouille *et al.*, 1995) was electroporated to MDCK cells that were grown under G418 selection for 2 wk before seeding the cell pool on filters. Characterization of MDCK cell clones stably expressing sialyltransferase will be described elsewhere (Scheiffele and Nilsson, unpublished data). The cells were SLO permeabilized as described above and double stained with AD7 and anti-VSV G, which were visualized by rhodamine and fluorescein isothiocyanate-conjugated secondary antibodies, respectively. Cells on filters were viewed with the EMBL confocal microscope. Image analysis was performed by using the Adobe Photoshop program. Images for figures were contrast enhanced in the Adobe Photoshop program and figures were digitally printed by using a dye sublimation printing process (Kodak, Rochester, NY).

Western Blot Analysis

Cytosol depletion of filter-grown MDCK cells was as described above. Immediately after the depletion the cells were lysed in 0.2% SDS, 2% NP-40 in PBS in the presence of protease inhibitors (chymostatin, leupeptin, antipain, and pepstatin, at 25 μg/ml each). Aliquots of permeabilized and intact cell lysates (10 μg protein) as well as cytosol from HeLa and MDCK cells (50 μg protein) were separated on 10% SDS-polyacrylamide gels. Proteins were transferred to a nitrocellulose membrane in 25 mM Tris, 190 mM glycine, and 20% methanol. Unspecific antibody binding was blocked by incubating the filter in 5% nonfat dried milk, 0.1% Tween 20 in PBS. The staining obtained with the AD7 hybridoma culture supernatant diluted in blocking solution was visualized using an HRP-conjugated secondary antibody and the enhanced chemiluminiscence detection system.

Preparation of MDCK Cytosol and Immunodepletion of p200

For cytosol preparation confluent MDCK monolayers from 60 150-cm^2 flasks were trypsinized, trypsin inactivated by first resuspending the cells back in culture medium and then, after pelleting, washing with 30 ml of 1 mg/ml soybean trypsin inhibitor in PBS. After washing away soybean trypsin inhibitor with ice-cold PBS the cell pellet was resuspended in cold swelling buffer (1 mM $MgCl_2$, 1 mM EGTA) and incubated on ice for 10 min. After pelleting the cells (1500 rpm, 10 min at 4°C), protease inhibitor cocktail (see above),

cytochalasin D (final 1 μM), and dithiothreitol (final 1 mM) were added and the cells broken by sonicating with a Branson sonifier using a 0.5-s pulse with microtip limit 6. The solution was then made isotonic in KOAc buffer (115 mM potassium acetate, 25 mM *N*-2-hydroxyethylpiperazine-*N'*-2-ethanesulfonic acid-KOH, pH 7.4, 2.5 mM $MgCl_2$) by adding KOAc buffer from a 10-fold concentrated stock solution. Following a 20-min centrifugation at 3000 rpm at 4°C the supernatant was centrifuged for 1 h at 75000 rpm at 4°C in TLA100.2 tubes in a Beckman table-top centrifuge (Fullerton, CA). The cytosol had a protein concentration of ~10 mg/ml and was stored aliquoted in liquid nitrogen. To deplete MDCK cytosol of p200, 15 μg of AD7 immunoglobulin G (IgG) was used for 100 μg of cytosol. In the control depletion the same amount of the monoclonal IgG P5D4 against VSV G was used. AD7 was concentrated from hybridoma culture supernatant by precipitating with 50% ammonium sulfate and purifying on a protein A column according to established procedures (Harlow and Lane, 1988). The purified IgG was coupled to protein A-Sepharose beads in PBS by rotating overnight at 4°C, the beads were washed with PBS containing 10% bovine serum albumin and then with KOAc-buffer, and cytosol was added to the beads and incubated for 3 h on ice with intermittent mixing. After spinning the beads down, the cytosol was filtered through a Millipore Ultrafree-MC filter (Bedford, MA) and used in the assay. Removal of p200 was monitored by SDS-PAGE and Coomassie staining of cytosol and eluate from the beads. When necessary a second round of immunodepletion was carried out. The depletion was quantitated by using the National Institutes of Health Image software.

In Vitro Transport Assays

The transport of VSV G and HA in SLO-permeabilized MDCK cells was carried out exactly as described previously (Pimplikar *et al.*, 1994; Ikonen *et al.*, 1995; for review see Lafont *et al.*, 1996). Briefly, polarized monolayers of MDCK cells on filter were infected with either VSV or influenza virus. After pulse labeling with [^{35}S]methionine the newly synthesized viral proteins were chased to the TGN using 20°C incubation. At this stage, one cell surface was permeabilized with SLO and the endogenous cytosol was depleted. Transport of the viral proteins from the TGN to the cell surface domains was reconstituted in a cytosol-, energy-, and temperature-dependent manner. The amount of viral proteins reaching the plasma membrane was measured by trypsinization (of HA) or immunoprecipitation (of VSV G). Quantitation of viral polypeptides resolved by SDS-PAGE was carried out using a PhosphorImager (Molecular Dynamics, Sunnyvale, CA). The values obtained with p200-depleted cytosol were expressed as a percentage of those given by mock-depleted cytosol (transport in the presence of control, i.e., mock-depleted cytosol being 100% and transport in the absence of added cytosol being 0%). Transport in the presence of mock-depleted cytosol was 1.7–2.5 fold higher than transport without cytosol addition and transport in the presence of untreated cytosol was 1.7–3.0 fold higher than transport without cytosol addition.

Resolution of Vesicles on Linear Equilibrium Density Gradients

MDCK cells on 10-cm diameter filters were metabolically labeled with [^{35}S]methionine, infected with fowl plague virus or VSV, and then incubated for 2 h at 20°C as described (Wandinger-Ness *et al.*, 1990), except that the labeling was not continued during the viral replication. Alternatively, cells were infected with either virus strain, the viral proteins were pulse labeled for 10 min with 150 μCi [^{35}S]methionine, and the cells were incubated for 2 h at 20°C. Perforation of cells, vesicle isolation, and pelleting the membranes through a sucrose cushion was done as described previously (Wandinger-Ness *et al.*, 1990) with the exception that 100 μM GMP-PNP was included both in the buffer after perforation and in the sucrose cushion. The membrane pellets were gently resuspended in 1 ml of 1.8 M sucrose in 10 mM *N*-2-hydroxyethylpiperazine-*N'*-2-ethanesulfonic acid-KOH, pH 7.4, 2 mM EGTA, 1 mM dithiothreitol, and 100 μM GMP-PNP and overlaid with a 0.5–1.7 M linear sucrose gradient in the same buffer. After centrifugation in SW40 rotor for 16 h at 35000 rpm, 1-ml fractions were collected from the top. Aliquots were taken for measuring the sucrose density and for analyzing the total protein pattern by SDS-PAGE after trichloroacetic acid (TCA) precipitation. From the fractions of the pulse-labeled samples proteins were TCA precipitated, and from the fractions of the metabolically labeled samples, p200 was immunoprecipitated with AD7 as described by Narula *et al.* (1992). The protein patterns were resolved on 10% (viral proteins) or 7% (p200) polyacrylamide gels.

Immunoelectron Microscopy

MDCK cells grown on 2.4-cm diameter filters were infected with influenza virus PR8 or VSV, incubated at 20°C, and perforated according to the method of Wandinger-Ness *et al.* (1990). The perforated cells were incubated in GGA-buffer in the presence of an ATP regenerating system (Wandinger-Ness *et al.*, 1990) and 100 μM GMP-PNP for 10 min at 37°C before fixing in 4% paraformaldehyde and 0.1% glutaraldehyde for 30 min. Small pieces were cut from the filters and incubated with 0.5% fish skin gelatin, 1% bovine serum albumin, and 0.1% glycine in PBS to block unspecific antibody binding. AD7 was incubated overnight at 4°C and after washing in blocking solution labeled with 10 nm protein A gold. After further washing the samples were incubated with 100 μg/ml protein A in PBS for 30 min, washed, fixed in 1% glutaraldehyde in PBS for 10 min, washed again, and incubated for 2 h at 37°C with the second antibody (anti-HA, anti-VSV G, or anti-Rab6), which was visualized with 5 nm protein A gold. The cells were then fixed in 0.5% glutaraldehyde in 100 mM cacodylate buffer, pH 7.35, for 30 min at room temperature, postfixed in an aqueous solution of 1% osmium containing 1.5% potassium ferrocyanide for 30 min at 4°C, and then treated with 1% tannic acid for 1 h at room temperature. After treatment with saturated uranyl acetate for 4–12 h at 4°C the cells were dehydrated and embedded in Epon resin. Sections were cut perpendicular to the substratum and stained with uranyl acetate and lead citrate before viewing in a Zeiss EM10 microscope. The ripped-off cell technique described above produced suboptimal labeling with all available anti-HA antibodies. To increase labeling for HA the perforated cells were incubated for 5 min at 37°C in GGA-buffer containing an ATP regenerating system and GMP-PNP as above, followed by 5 min at room temperature in the same mixture supplemented with 0.1% saponin. The cells were then fixed in 4% paraformaldehyde, labeled, and processed as described above. To quantitate the labelings the distribution of 200 gold particles for p200, 262 particles for VSV G, and 181 particles for HA were examined in the apical (peri-Golgi) areas of the cells. Vesicular profiles having two or more p200, VSV, or HA gold particles were scored as positive for the marker.

RESULTS

Recruitment of p200 from Cytosol to Golgi Membranes Is Regulated by G Proteins in MDCK Cells

The dynamics of p200 binding to membranes has been shown to share characteristics with known coat proteins. BFA caused dissociation of p200 from Golgi membranes in NRK cells, even more rapidly than that of β-COP. In the BFA-resistant cell line PtK_1, BFA failed to cause redistribution of p200 (Narula *et al.*, 1992). On the other hand, p200 membrane association could be enhanced by treatments that activate heterotrimeric G proteins, e.g. with aluminium fluoride

(AlF_4-) or mastoparan (de Almeida *et al.*, 1993). We first analyzed by immunocytochemistry whether the membrane association of p200 in MDCK cells is sensitive to these treatments. In MDCK cells, the perinuclear p200 staining visualized by the monoclonal antibody AD7 was not altered in the presence of BFA (Figure 1, A and B) although the same treatment completely shifted p200 to the cytosolic pool in BHK cells (Figure 1, C and D). This is in line with the observation that the organization of the Golgi complex as well as the membrane binding of β-COP are resistant to BFA exposure in MDCK cells (Hunziker *et al.*, 1991). However, the treatment of MDCK cells with AlF_4- induced translocation of p200 from the cytoplasm onto the Golgi complex as visualized by the disappearance of the diffuse cytosolic staining and more intense perinuclear immunoreactivity (Figure 1E). Thus, the regulation of p200 membrane

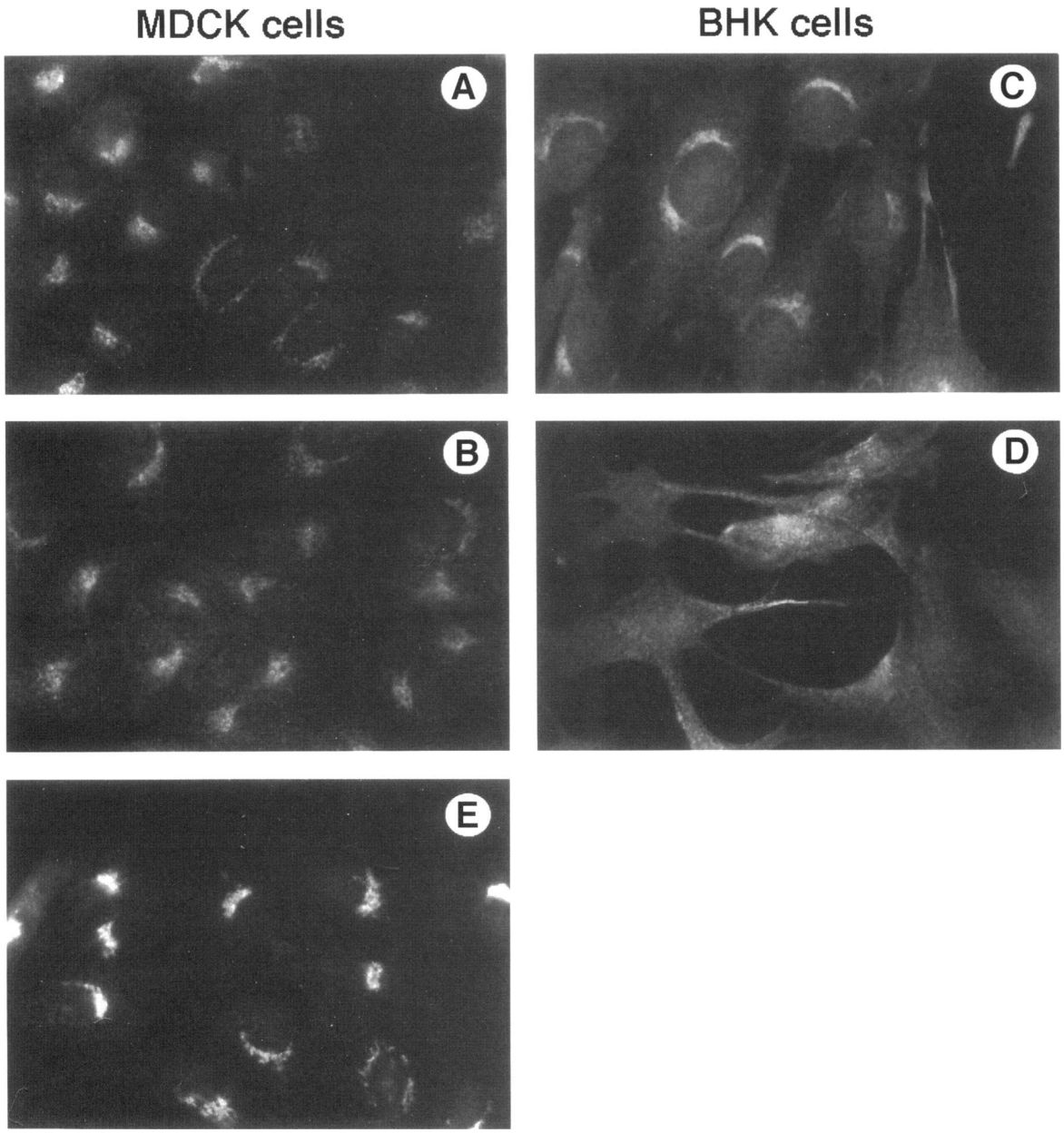

Figure 1. Effect of BFA and AlF_4- on the distribution of p200 in MDCK cells. MDCK cells (A, B, and E) and BHK cells (C and D) were grown on coverslips and stained with the AD7 antibody without drug treatments (A and C), after 5 min treatment with 5 μg/ml of BFA (B and D) or after 30 min treatment with AlF_4- (50 μM $NH_4Al(SO_4)_2$ and 10 mM KF) (E).

binding by heterotrimeric G proteins seems to be maintained in MDCK cells.

Immunodepletion of p200 from MDCK Cytosol

In filter-grown confluent MDCK cell monolayers the p200 antibody gave a strong but more diffuse staining than in plastic-grown cells (compare Figure 1A with Figure 2A). When the cells were permeabilized from either the basolateral (Figure 2, B and C) or apical (our unpublished results) surface with SLO and the endogenous cytosol depleted, the staining disappeared almost completely. This loss of p200 from the cells could partially be prevented if the cells were incubated with a nonhydrolyzable GTP-analogue GMP-PNP during cytosol depletion. Under these conditions the residual staining was more clearly perinuclear (compare Figure 2, D and E with B and C), suggesting preferential association of p200 with Golgi membranes. This was confirmed by colocalization of p200 and the resident TGN marker sialyltransferase in the perinuclear structures (Figure 2, E and F). As efficient removal of p200 is crucial for functional studies on the effect of p200 depletion, we confirmed the disappearance of p200 from SLO-permeabilized MDCK cells by Western blot analysis. In accordance with the immunocytochemical results, no p200 was detected in cells permeabilized from either plasma membrane domain (Figure 3A).

For in vitro transport assays in MDCK cells we routinely use HeLa cytosol because of its ease of preparation and its efficiency, which is comparable to that of MDCK cytosol in supporting transport (Pimplikar *et al.*, 1994). In HeLa cytosol the p200 antibody, however, recognizes only a 250-kDa cross-reactive protein (Figure 3B). Since the identity of this protein is not clear (Narula *et al.*, 1992) we decided to use MDCK cytosol in the transport assays (Figure 3B). The AD7 antibody immunoprecipitates p200 (Narula *et al.*,

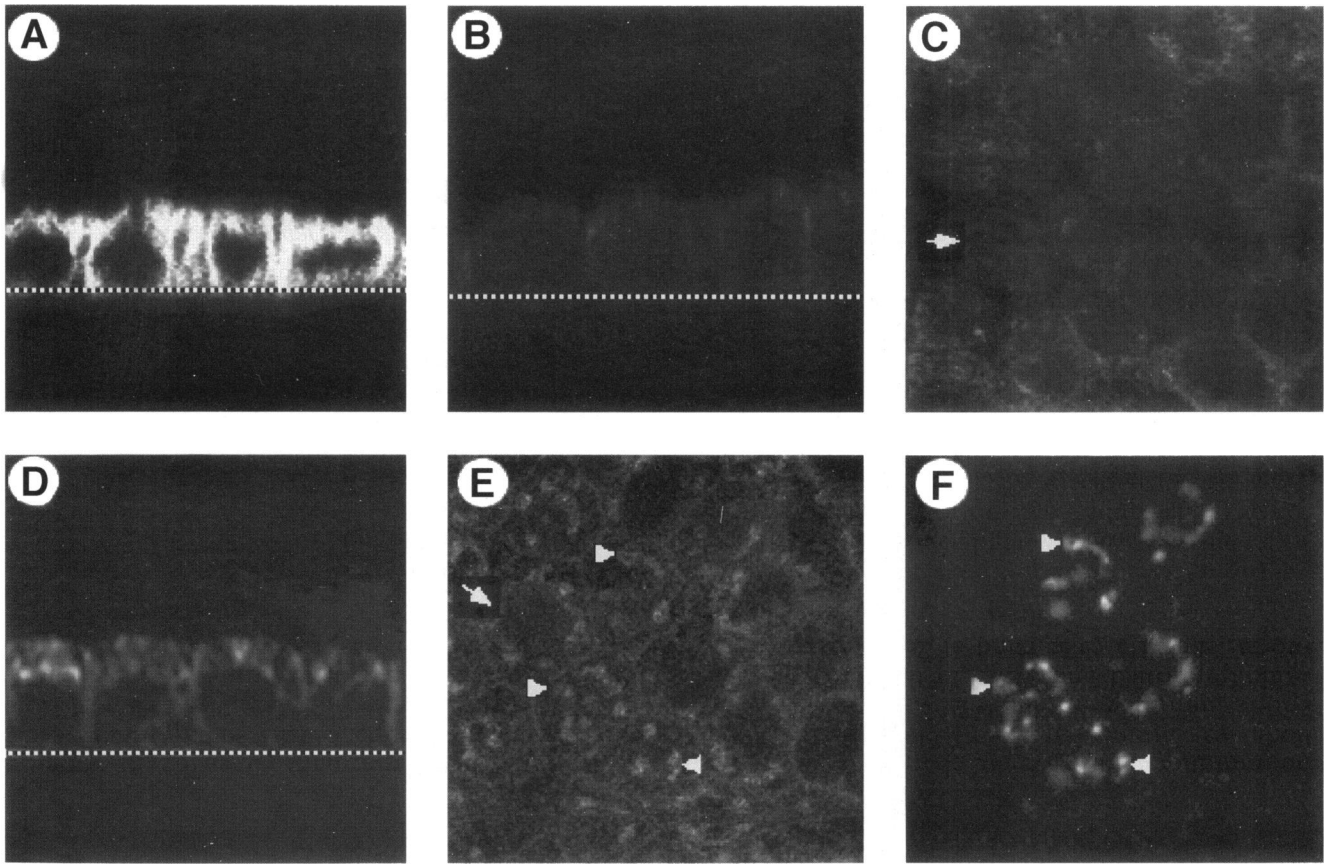

Figure 2. Depletion of p200 from filter-grown MDCK cells after SLO-permeabilization and cytosol depletion. Filter-grown MDCK cells were labeled with AD7 without SLO permeabilization (A) and after SLO permeabilization of the basolateral surface and cytosol depletion (B and C). (D–F) The same surface was SLO permeabilized and cytosol depleted in the presence of 100 μM GMP-PNP. (D and E) Labeling with AD7; (F) the same field as in panel E, showing labeling of VSV G-tagged sialyltransferase expressing cells with anti-VSV G antibody. (A, B, and D) Confocal z sections; (C) an x,y section corresponding to panel B; (E and F) x,y sections corresponding to panel D. The levels of the sections are indicated by arrows. Arrowheads indicate the perinuclear punctate staining visualized in the presence of GMP-PNP.

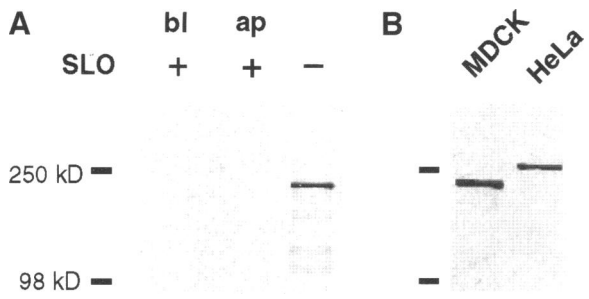

Figure 3. Western blot analysis of MDCK cell lysates, MDCK cytosol, and HeLa cytosol using AD7. (A) Intact filter-grown MDCK cells and MDCK cells where cytosol had been depleted after SLO-permeabilization either from the apical or basolateral side, were lysed and identical amounts of cellular proteins were separated by SDS-PAGE and blotted with the AD7 antibody. (B) Identical amounts of MDCK and HeLa cytosol were separated by SDS-PAGE and blotted with AD7.

1992) and could therefore be used to efficiently immunodeplete the protein from MDCK cytosol. In spite of its abundance over 98% of p200 could be depleted (Figure 4).

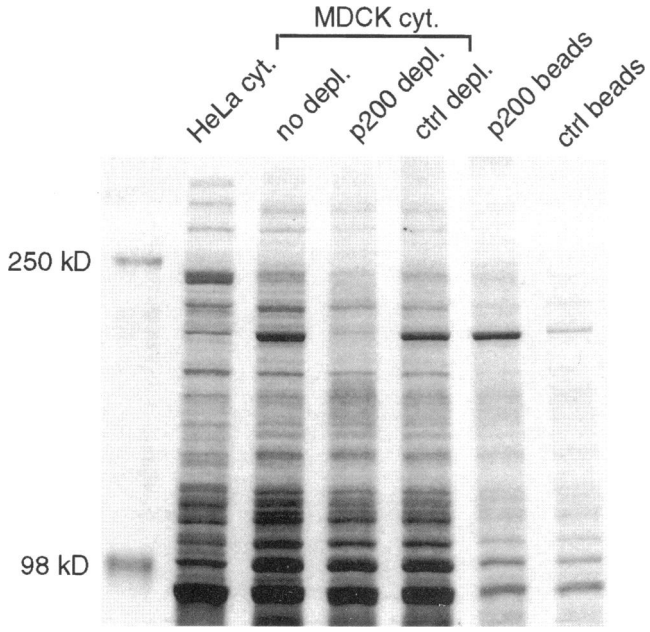

Figure 4. Immunodepletion of p200 from MDCK cytosol. MDCK cytosol was incubated with protein A-Sepharose beads where either AD7 or an irrelevant antibody P5D4 had been coupled. Aliquots of the p200 and mock-depleted cytosols as well as of protein recovered from the beads were resolved by SDS-PAGE and stained with Coomassie brilliant blue. For comparison, the protein pattern of HeLa cytosol is also shown.

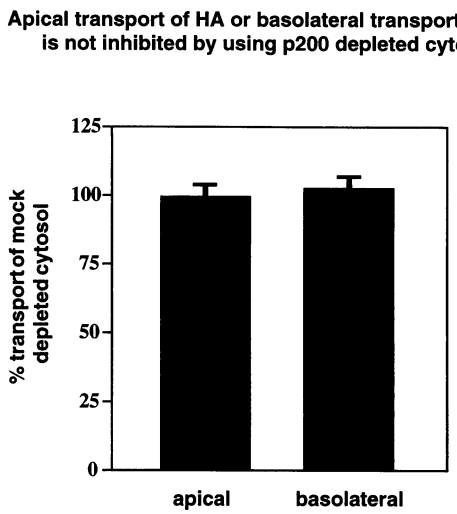

Figure 5. In vitro transport of HA and VSV G is not inhibited by using p200-depleted cytosol. Apical and basolateral transport assays were carried out in SLO-permeabilized MDCK cells by using p200-depleted MDCK cytosol or MDCK cytosol mock depleted with an irrelevant monoclonal antibody. Transport obtained in the presence of mock-depleted cytosol was scored as 100% and transport without cytosol addition as 0% transport. The values represent means ± SEMs of three assays performed with duplicate filters. Transport in the presence of mock-depleted cytosol was 90% of that observed with untreated cytosol.

Apical Transport of HA or Basolateral Transport of VSV G Is not Affected by Depletion of p200

The in vitro transport assays established in our laboratory to study exocytic trafficking from the TGN to the apical and basolateral plasma membrane domains are based on filter-grown MDCK cells permeabilized with the bacterial toxin SLO (Kobayashi *et al.*, 1992; Pimplikar and Simons, 1993; Pimplikar *et al.*, 1994; Ikonen *et al.*, 1995; Lafont *et al.*, 1996). Under the assay conditions transport of a viral marker protein–HA transported to the apical surface or VSV G delivered to the basolateral surface–is ATP and temperature dependent and requires the substitution of depleted cytosol with exogenous cytosolic proteins. Based on the fact that p200 leaked completely out from SLO-permeabilized cells and that we could efficiently deplete it from the exogenously added MDCK cytosol, we tested whether transport to the cell surface is dependent on p200. No differences were detected between the p200 and mock-depleted cytosols in the efficiency to support transport of HA from the TGN to the apical surface or transport of VSV G from the TGN to the basolateral surface (Figure 5).

p200-Containing Vesicles Have a Higher Density than Apical and Basolateral Vesicles

Previous work from our laboratory has shown that the apical and basolateral vesicles released from mechan-

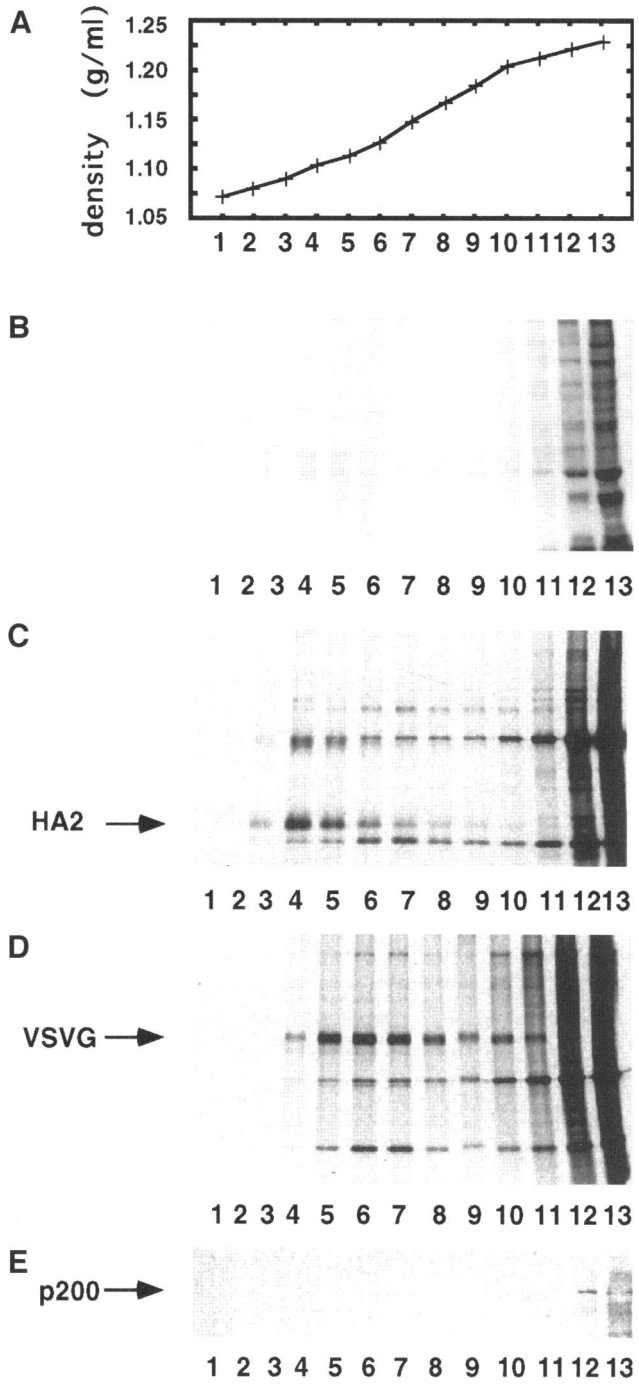

Figure 6. HA, VSV G, and p200 containing vesicles have different equilibrium densities. The membrane pellets isolated from pulse-labeled fowl plague virus (C) or VSV (D)-infected MDCK cells were resuspended in 1.8 M sucrose and overlaid with a 0.5–1.7 M linear sucrose gradient. After centrifugation to equilibrium fractions were collected from the top and the proteins TCA precipitated from each fraction. HA2 is proteolytically cleaved from fowl plague virus HA during exit from the TGN (Wandinger-Ness *et al.*, 1990). To localize p200-containing membranes, membrane pellets isolated from metabolically labeled and virally infected MDCK cells were separated on an identical gradient and p200 immunoprecipitated from each fraction with AD7 (E). The proteins were resolved by SDS-PAGE and stained with Coomassie brilliant blue to visualize the total protein pattern after TCA-precipitation (B) or analyzed by fluorography (C–E).

ically perforated MDCK cells have different equilibrium densities, the VSV G-containing vesicles being slightly heavier (vesicle peak corresponding to a density of 1.113 g/ml in a sucrose gradient) than the HA2-containing vesicles (peaking at 1.099 g/ml) (Wandinger-Ness *et al.*, 1990). To test whether p200 is present on either vesicle type we perforated virally infected filter-grown MDCK cells using a nitrocellulose filter and collected the material released from the cells (Wandinger-Ness *et al.*, 1990). After concentration the membranes were overlaid with a linear 0.5–1.7 M sucrose gradient and floated to their equilibrium densities. To promote membrane association of p200, GMP-PNP was included in all solutions after the perforation. Analysis of the marker proteins on gradient fractions revealed that the marker for apical vesicles, HA2, peaked at the density corresponding to 1.104 g/ml (Figure 6C, fraction 4). The basolateral vesicle marker VSV G was, as expected, most enriched in slightly denser fractions, peaking at the density corresponding to 1.132 g/ml (Figure 6D, fraction 6). When p200 was detected in the fractions either by immunoprecipitation (Figure 6E) or by Western blotting (our unpublished results) the most intense signal was obtained from the fractions having the highest density (1.219–1.230 g/ml, Figure 6E, fractions 12 and 13). This suggested that the majority of p200 did not migrate from the loading zone because it was associated with membranes the density of which is clearly higher than those of apical and basolateral vesicles. It is also conceivable that the location of p200 does not reflect the true density of p200-containing carriers because p200 formed aggregates or dissociated from the membrane. Therefore, we repeated the experiment using a linear gradient of higher density, from 1.0 to 2.2 M sucrose. In this gradient p200 was not only immunoprecipitated from the heaviest fractions but it could be recovered from fractions corresponding to the density of 1.230 g/ml (our unpublished results). These results speak in favor of p200 associating with membranes that are denser than those budding from the TGN and harboring HA and VSV G.

p200 Does Not Colocalize with HA or VSV G in the TGN-derived Vesicles

In electron microscopic studies p200 has been localized to the cytoplasmic surface of non-clathrin–coated vesicles in the TGN. These vesicles were different from the β-COP containing Golgi-derived vesicles and often contained TGN38 in addition to p200 (Narula and Stow, 1995).

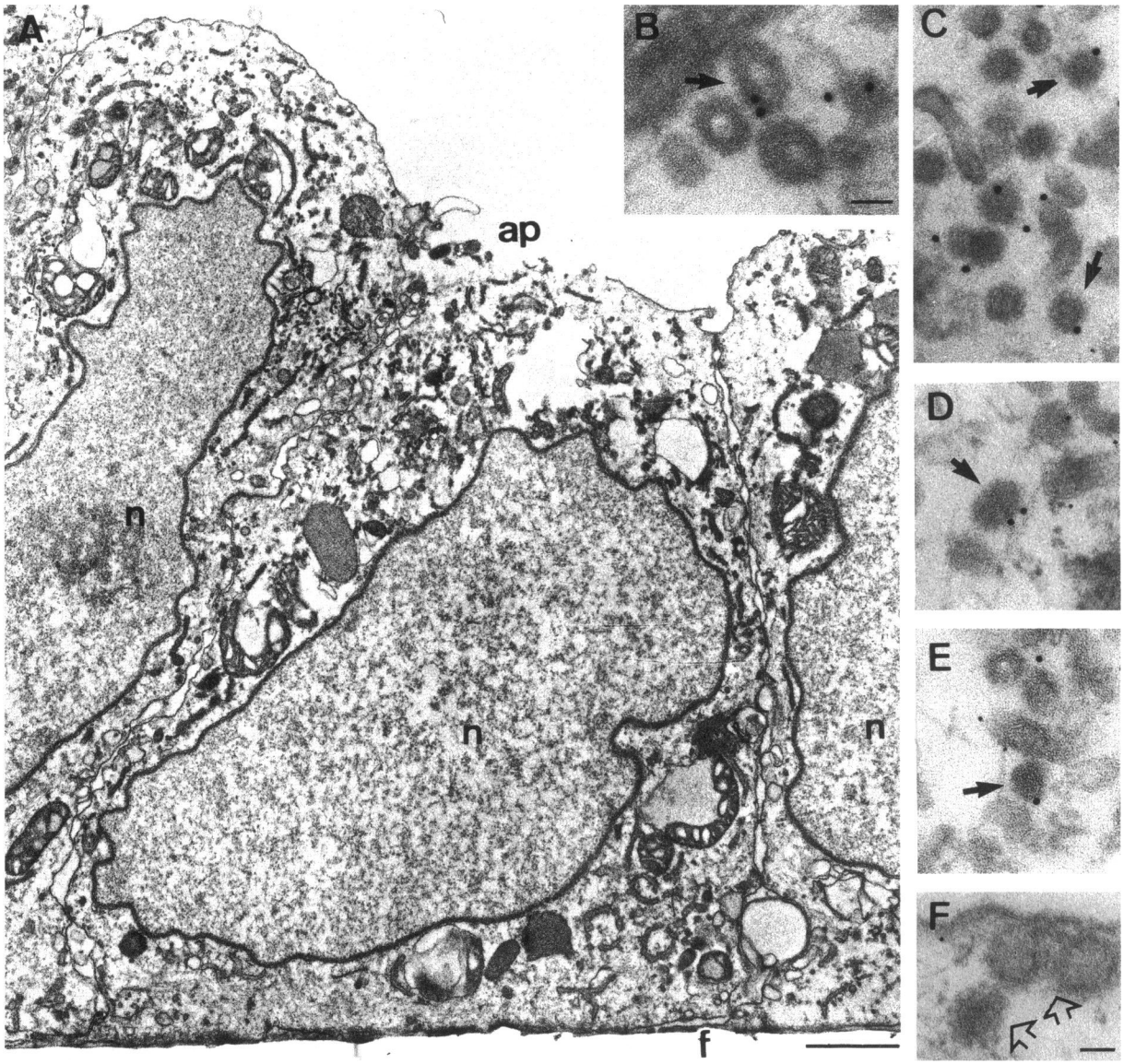

Figure 7. Ultrastructure of perforated MDCK cells and p200 positive vesicles. MDCK cells were infected with VSV, incubated at 20°C to accumulate the VSV G protein in the TGN, and then perforated. After a 10-min incubation at 37°C in the presence of GMP-PNP the cells were fixed and labeled for p200 (large [10 nm] gold) and VSV G (small [5 nm] gold). (A) A low power overview showing the ultrastructure of the perforated cells. Despite holes in the apical surface (ap) the intracellular organelles appear to be well preserved. (B–E) Labeling for p200 is associated with vesicles with a thin electron dense cytoplasmic coat. The coat is clearly distinct from that of clathrin-coated vesicles shown in panel F. In this and subsequent figures (8, 9, and 10) clathrin-coated vesicles are indicated by open arrows, and p200-positive vesicles by small broad arrows. f, filter; n, nucleus. Bars: panel A, 1 μm; panels B and F, 50 nm (C–F at the same magnification).

We have established conditions where the morphology of the perforated cells is well preserved at the electron microscopic level and efficient labeling of the intracellular structures with antibodies can be achieved. This technique has the advantage that small transport vesicles and any associated coats are clearly visualized. Using this technique, we analyzed the distribution of p200 and compared it with that of viral marker proteins arrested in the TGN using a 20°C block. The cells were perforated after the temperature block and incubated shortly at 37°C in the presence of GMP-PNP before fixation and antibody labeling. Although the apical plasma membrane was perforated and the cytosol depleted, the general ultrastructure of the cells was well maintained (see Figure 7, which shows cells after a double labeling experiment). Intracellular organelles such as endosomes, the Golgi complex, and the endoplasmic reticulum were retained

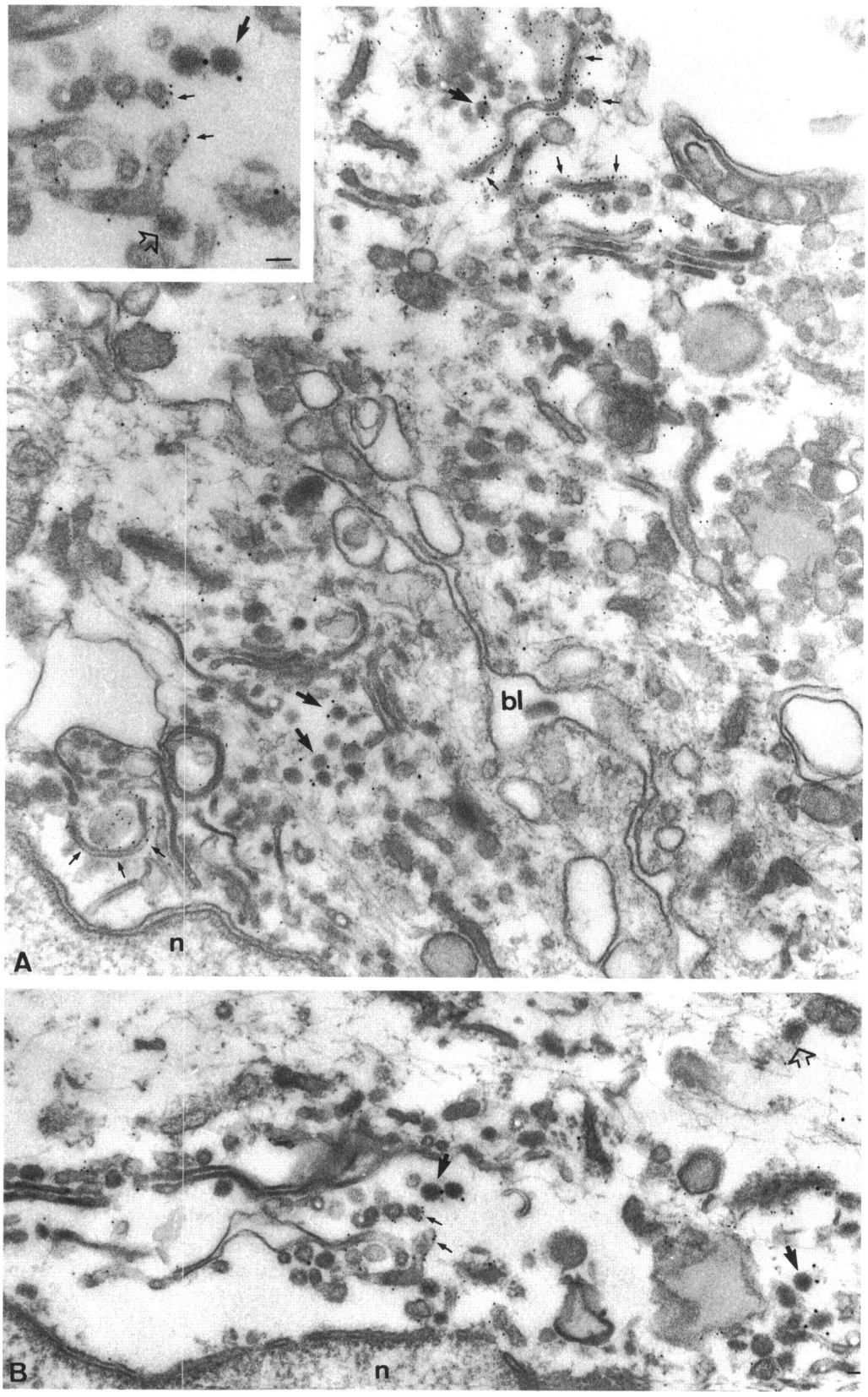

Figure 8. Double labeling of VSV-infected perforated cells for p200 and VSV G. MDCK cells infected with VSV were incubated and labeled for p200 (large gold) and VSV G (small gold) as described in the legend to Figure 7. p200 labeling is associated with vesicular profiles with an electron dense coat (large arrows) that do not show heavy labeling for VSV G. The VSV G labeling is highly concentrated in tubular or cisternal elements and vesicular profiles (small arrows, see in particular upper right region of panel A and inset). These elements show low labeling for p200 and are less electron dense. Open arrows indicate clathrin-coated vesicles. n, nucleus; bl, basolateral membrane. Bar, 50 nm.

inside the cells, consistent with previous biochemical results (Wandinger Ness *et al.*, 1990). The short warming up period allowed the accumulation of several types of small transport vesicles in the cytoplasm (Figure 7). In addition to clathrin-coated vesicles other, as yet unidentified, coated vesicles could also be found in the Golgi region. The p200 antibody predominantly labeled the surface of characteristic coated vesicular profiles of diameter between 50 and 60 nm. These profiles, corresponding to buds or free vesicles, displayed a cytoplasmic coat of approximately 10 nm that was thinner, but more electron dense, than that of clathrin-coated vesicles. This coat gave the entire vesicle a more electron dense appearance than other vesicles in the Golgi region. Uncoated tubular structures in the TGN area were also labeled by the p200 antibody. Double labeling was performed using antibodies to p200 and VSV G (Figure 8) or HA (Figure 9). For the latter a saponin extraction was required to maximize labeling but similar results were obtained without detergent (results not shown). The viral antigens labeled tubular, cisternal, or vesicular elements that were predominantly on one side of the Golgi stack. The endoplasmic reticulum and the bulk of the Golgi cisternae showed low labeling under these conditions. The p200-positive vesicles or buds were not significantly labeled by antibodies to the viral proteins and the p200-decorated vesicles were clearly more electron dense than the ones labeled most heavily with the viral markers (Figure 8). However, p200 was occasionally found in the same tubular elements of the TGN as the viral markers (Figure 8). Quantitation of double labeling experiments for p200 and VSV G revealed that 76% of p200 gold particles were associated with electron dense vesicular profiles. Of these 98% were negative for VSV G. In the case of p200 and HA double labeling, 74% of p200 gold particles were associated with electron dense vesicular profiles and 99% of these were HA negative.

Previously, p200 was shown to colocalize with TGN38 on the same or closely adjacent vesicles (Narula and Stow, 1995). TGN38 is known to associate with a cytosolic complex of Rab6 and p62, this interaction playing an essential role in vesicle budding (Jones *et al.*, 1993). If p200 can participate in this complex formation it should be possible to visualize at least partially overlapping distributions of p200 and Rab6. Double labeling of perforated cells with p200 and Rab6 antibodies demonstrated that this indeed was the case (Figure 10). Although Rab6 was not enriched on the p200-positive buds, these buds were often attached to Rab6-positive cisternae. Since Rab6 has not been implicated in apical or basolateral transport (Huber *et al.*, 1993; Martinez *et al.*, 1994) this provides further evidence for the different identity of p200 vesicles.

DISCUSSION

Given the TGN localization of p200 and the fact that no coat proteins have been identified for vesicles trafficking from the TGN to the plasma membrane we decided to test whether p200 could be a coat protein of either apical or basolateral vesicles. The molecular identity of the protein remains unknown and no functional data are available.

We took several independent approaches to analyze the relation of p200 to the apical and basolateral marker proteins. First, p200 could not be visualized in floated membrane fractions containing the viral markers. Second, p200 localized to electron dense vesicles and tubules associated with the TGN also in MDCK cells but it was not seen in the same vesicular structures that labeled for HA or VSV G. Third, the delivery of HA or VSV G from the TGN to the cell surface was not affected when p200 was removed from the cells. Theoretically it is possible that the trace amounts of p200 potentially left in the cell might be sufficient to support transport if p200 was normally available in vast excess or that the p200 dependent step has already been passed when initiating transport. It could also be envisaged that the labeling of membrane with p200 antibody would somehow sterically hinder the viral proteins from being labeled in the vicinity of p200. However, single labeling experiments with antibodies against the viral glycoproteins showed no significant labeling of vesicles with the morphology of the p200 profiles (our unpublished observations). Taken together, the simplest explanation of our results is that p200 does not form the coat of apical or basolateral vesicles transporting HA and VSV G, respectively. In accordance with this, we have analyzed the high molecular weight range in the protein composition of apical and basolateral vesicles immunoisolated in the presence of GMP-PNP and have been unable to detect p200 on either vesicle type (our unpublished results).

It is evident that several distinct vesicle populations can be generated from the Golgi apparatus (Griffiths *et al.*, 1985; Orci *et al.*, 1986; Ladinsky *et al.*, 1994). At least COPI, clathrin, and p200-coated vesicles bud from the Golgi membranes, yet none of these coat proteins are likely to participate in the formation of apical or basolateral vesicles. We have shown that the addition of cytosol increases the budding of apical and basolateral vesicles from perforated MDCK cells (Pimplikar *et al.*, 1994). Whether these cytosolic factors are proteins assembling as a scaffold on the budding membrane to drive vesicle formation remains open. The finding that BFA affects both apical and basolateral sorting suggests that coat proteins are involved (Matter *et al.*, 1993; Wagner *et al.*, 1994). However, we could not observe major changes in the densities of either vesicle population upon incubation with GMP-PNP, which

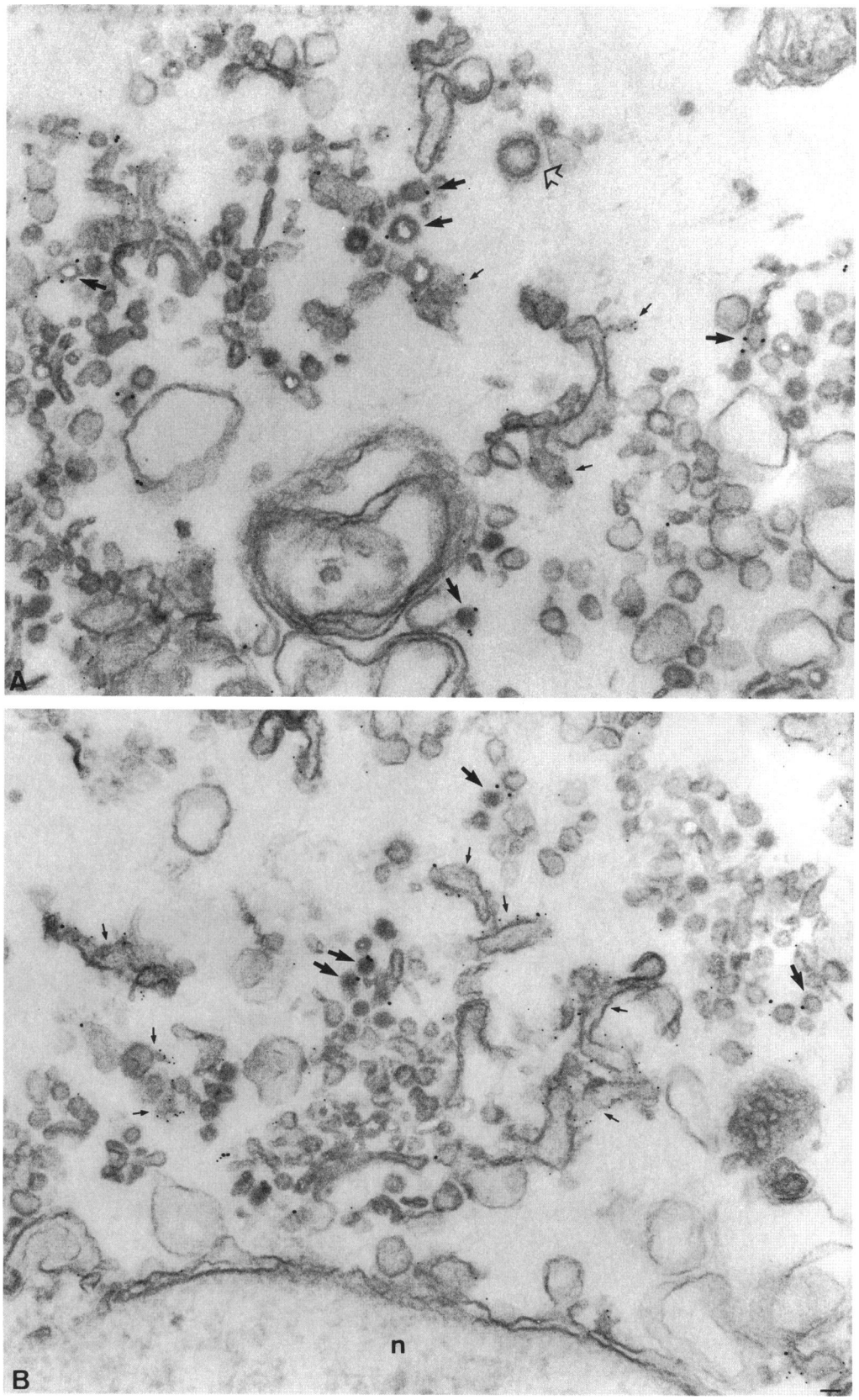

Figure 9. Double labeling of influenza virus-infected perforated cells for p200 and HA. MDCK cells were infected with influenza virus and newly synthesized HA accumulated in the TGN at 20°C. The cells were then perforated and incubated for 5 min at 37°C in the presence of GMP-PNP followed by 5 min at room temperature in the presence of 0.1% saponin and GMP-PNP. The cells were fixed and labeled with antibodies to p200 (large gold) and to the cytoplasmic domain of HA (small gold). Despite the poorer membrane preservation due to the saponin treatment, the typical morphology of the p200-positive electron dense vesicles is still apparent (large arrows). These vesicles show low labeling for HA, which is mainly concentrated within cisternal elements (small arrows) that show lower labeling for p200. Open arrow indicates a clathrin-coated vesicle. n, nucleus. Bar, 50 nm.

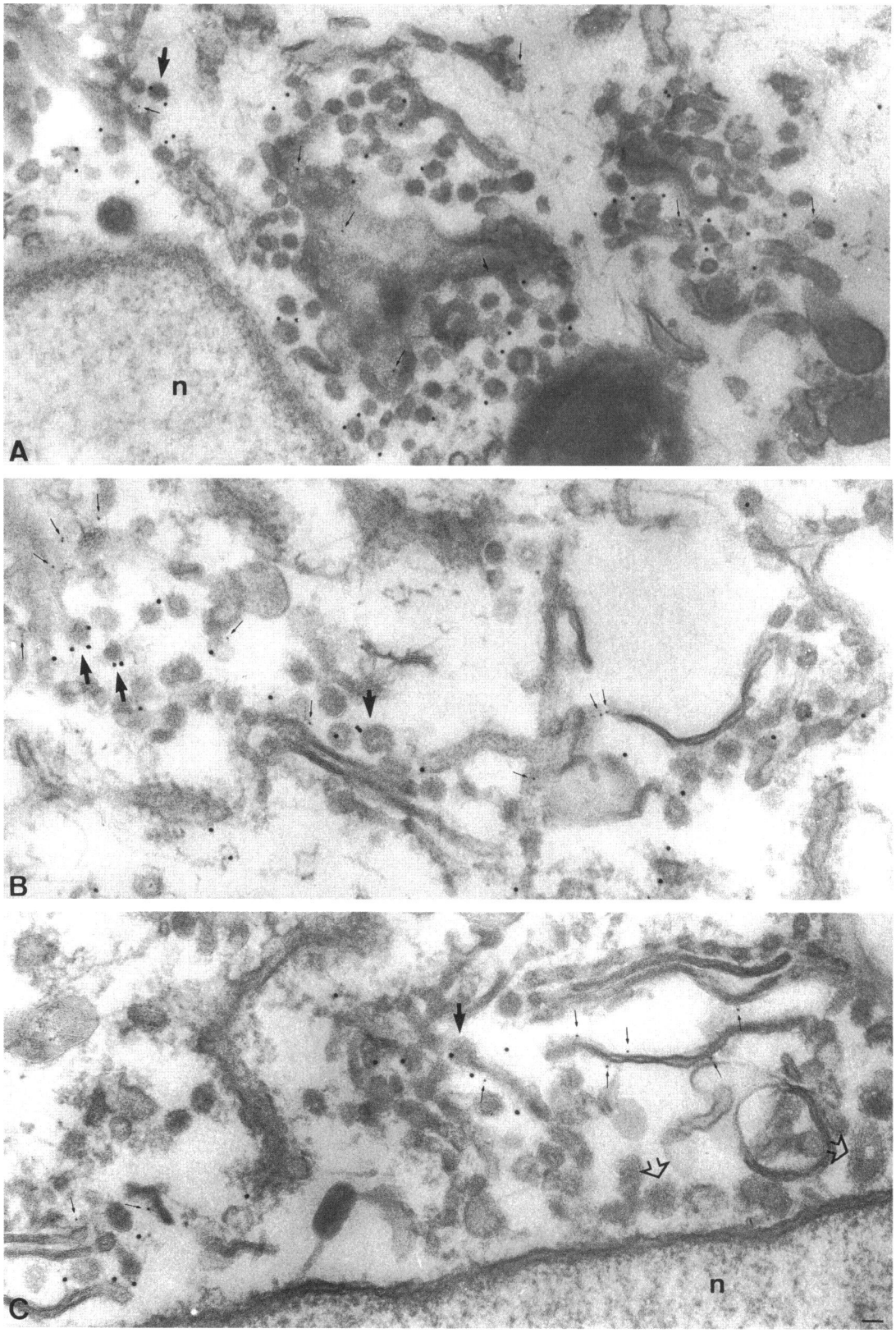

Figure 10.

could be viewed as potential evidence against coats on these vesicles. On the other hand, these data may equally well be explained by a putative coat not remaining efficiently fixed to the vesicles by preventing GTP hydrolysis, or the density shift caused by the addition of a coat being too small to be detected on density gradients. It is evident from our results that if apical and basolateral vesicles carry coats, they are morphologically not as readily identifiable as the characteristic cages of clathrin-coated vesicles or the electron dense coat of p200 vesicles with the electron microscopic technique that we used.

If p200-containing transport vesicles form in the TGN–as is reasonable to expect based on the localization of p200 on membrane buds in the TGN–and the protein is not involved in the budding of apical or basolateral vesicles in MDCK cells, what other destinations could it be targeted to? Recent results have provided evidence for several exocytic routes to the cell surface even in simple eukaryotes (Harsay and Bretscher, 1995) and for several vesicle types trafficking from the TGN to the same specialized cell surface domain in polarized epithelial cells (Saucan and Palade, 1994). Therefore, it is conceivable that yet alternative routes to the ones used by the viral proteins lead from the TGN to the plasma membrane domains in MDCK cells, and p200 could be functioning in such a pathway. The involvement of p200 in transport routes connecting the TGN to the endosomes also remains a possibility even though our results clearly confirm the earlier finding that p200 is not present on clathrin-coated vesicles (Narula and Stow, 1995). The partial colocalization we observed with p200 and Rab6, on the other hand, could also point to the possibility that p200 participates in intra-Golgi trafficking (Martinez *et al.*, 1994). In this case it should function in a route distinct from COPI-coated vesicles as p200 does not colocalize with β-COP (Narula and Stow, 1995). Since Rab6 has been suggested either to exert an inhibitory effect on anterograde transport or to regulate backward trafficking within the Golgi complex, p200 could have a role in retrograde membrane transport from the TGN.

Further insight into the identity of p200 vesicles and the molecular components interacting with p200 can now be gained by using the AD7 antibody to immunoisolate p200-decorated vesicular carriers and by analyzing their protein composition. Moreover, the observed abundance of p200 among MDCK cytosolic proteins will make the purification of the protein feasible in sufficient quantities to enable molecular cloning and characterization of the protein.

Figure 10 (cont). Double labeling of perforated cells for p200 and Rab6. MDCK cells were incubated at 20°C, perforated, and further incubated at 37°C in the presence of GMP-PNP. They were then labeled for p200 (large gold) and Rab6 (small gold). Rab6 is mainly associated with cisternal elements, often with a typical TGN-appearance (e.g. see panel A). The p200-positive vesicular profiles and buds (large arrows) are usually negative for Rab6 (gold particles indicated by small arrows) but are often continuous with the Rab6-positive cisternae (see for example, p200-positive bud to left of panel B, and bud indicated by arrow in center of panel C). n, nucleus. Bar, 50 nm.

ACKNOWLEDGMENTS

The authors thank Karl Matlin (Harvard Medical School, Boston, MA) for providing the hybridoma cells producing AD7, Bruno Goud (Institut Curie, Paris, France) for kindly providing the anti-Rab6 antibody, and Sucharit Bhakdi (University of Mainz, Mainz, Germany) for the generous supply of SLO. We are grateful to Kathryn Howell (University of Colorado, Denver, CO) for giving helpful advice and for sharing unpublished results. We thank Tommy Nilsson (European Molecular Biology Laboratory, Heidelberg, Germany) for providing the sialyltransferase cDNA and the anti-VSV G antibody as well as for critical reading of the manuscript. We are grateful to Peter Scheiffele for MDCK cells expressing tagged sialyltransferase, Hilkka Virta and Brigitte Joggerst for excellent technical assistance throughout the study, and Sandra Ruf for cytosol preparation. This work was financially supported by the Commission of the European Communities (H.C.M. fellowships to E.I. and F.L.), the Academy of Finland, and the Deutche Forschungsgemeinschaft (SFB 352).

REFERENCES

Barlowe, C., Orci, L., Yeung, T., Hosobuchi, M., Hamamoto, S., Salama, N., Rexach, M.F., Ravazzola, M., Amherdt, M., and Schekman, R. (1994). COPII: a membrane coat formed by Sec proteins that drive vesicle budding from the endoplasmic reticulum. Cell *77*, 895–907.

Bennett, M.K., Wandinger-Ness, A., and Simons, K. (1988). Release of putative exocytic transport vesicles from perforated MDCK cells. EMBO J. *7*, 4075–4085.

de Almeida, J.B., Doherty, J., Ausiello, D.A., and Stow, J.L. (1993). Binding of the cytosolic p200 protein to Golgi membranes is regulated by heterotrimeric G proteins. J. Cell Sci. *106*, 1239–1248.

Fiedler, K., Lafont, F., Parton, R.G., and Simons, K. (1995). Annexin XIIIb: a novel epithelial-specific annexin is implicated in vesicular traffic to the apical plasma membrane. J. Cell Biol. *128*, 1043–1053.

Fiedler, K., Parton, R.G., Kellner, R., Etzold, T., and Simons, K. (1994). VIP36, a novel component of glycolipid rafts and exocytic carrier vesicles in epithelial cells. EMBO J. *13*, 1729–1740.

Griffiths, G., Pfeiffer, S., Simons, K., and Matlin, K. (1985). Exit of newly synthesized membrane proteins from the trans cisternae of the Golgi complex to the plasma membrane. J. Cell. Biol. *101*, 949–964.

Harlow, E., and Lane, D. (1988). Antibodies: A Laboratory Manual, Cold Spring Harbor, NY: Cold Spring Harbor Laboratory Press.

Harsay, E., and Bretscher, A. (1995). Parallel secretory pathways to the cell surface in yeast. J. Cell Biol. *131*, 297–310.

Huber, L.A., Pimplikar, S., Parton, R.G., Virta, H., Zerial, M., and Simons, K. (1993). Rab8, a small GTPase involved in vesicular traffic between the TGN and the basolateral plasma membrane. J. Cell Biol. *123*, 35–45.

Hughson, E., Wandinger-Ness, A., Gausepohl, H., Griffiths, G., and Simons, K. (1988). The Cell Biology of Enveloped Virus Infection of Epithelial Tissues, ed. M. Schwartz, Paris, France: Elsevier, 75–89.

Hunziker, W., Whitney, A., and Mellman, I. (1991). Selective inhibition of transcytosis by brefeldin A in MDCK cells. Cell *67*, 617–627.

Ikonen, E., Tagaya, M., Ullrich, O., Montecucco, C., and Simons, K. (1995). Different requirements for NSF, SNAP, and rab proteins in apical and basolateral transport in MDCK cells. Cell *81*, 571–580.

Jamieson, J.D., and Palade, G.E. (1967). Intracellular transport of secretory proteins in the pancreatic exocrine cell. 1: Role of the peripheral elements of the Golgi complex. J. Cell Biol. *34*, 577–596.

Jones, S.M., Crosby, J.R., Salamero, J., and Howell, K.E. (1993). A cytosolic complex of p62 and rab6 associates with TGN38/41 and is involved in budding of exocytic vesicles from the trans-Golgi network. J. Cell Biol. *122*, 775–788.

Kobayashi, T., Pimplikar, S., Parton, R.G., Bhakdi, S., and Simons, K. (1992). Sphingolipid transport from the trans-Golgi network to the apical surface in permeabilized MDCK cells. FEBS Lett. *300*, 227–231.

Kreis, T.E. (1986). Microinjected antibodies against the cytoplasmic domain of vesicular stomatitis virus glycoprotein block its transport to the cell surface. EMBO J. *5*, 931–941.

Kurzchalia, T.V., Dupree, P., Parton, R.G., Kellner, R., Virta, H., Lehnert, M., and Simons, K. (1992). VIP21, a 21-kD membrane protein is an integral component of trans-Golgi network–derived transport vesicles. J. Cell Biol. *118*, 1003–1014.

Ladinsky, M.S., Kremer, J.R., Furcinitti, P.S., McIntosh, J.R., and Howell, K.E. (1994). HVEM tomography of the trans-Golgi network: structural insights and identification of a lace-like vesicle coat. J. Cell Biol. *127*, 29–38.

Lafont, F., Simons, K., and Ikonen, E. (1996). Dissecting the molecular mechanisms of polarized membrane traffic: reconstitution of three transport steps in epithelial cells using streptolysin O permeabilization. Cold Spring Harbor Symp. Quant. Biol. (*in press*).

Letourneur, F., Gaynor, E.C., Hennecke, S., Demolliere, C., Duden, R., Emr, S.D., Riezman, H., and Cosson, P. (1994). Coatomer is essential for retrieval of dilysine-tagged proteins to the endoplasmic reticulum. Cell *79*, 1199–1207.

Martinez, O., Schmidt, A., Salamero, J., Hoflack, B., Roa, M., and Goud, B. (1994). The small GTP-binding protein rab6 functions in intra-Golgi transport. J. Cell Biol. *127*, 1575–1588.

Matter, K., Whitney, J.A., Yamamoto, E.M., and Mellman, I. (1993). Common signals control low density lipoprotein receptor sorting in endosomes and the Golgi complex of MDCK cells. Cell *74*, 1053–1064.

Narula, N., McMorrow, I., Plopper, G., Doherty, J., Matlin, K.S., Burke, B., and Stow, J.L. (1992). Identification of a 200-kD, brefeldin-sensitive protein on Golgi membranes. J. Cell Biol. *117*, 27–38.

Narula, N., and Stow, J.L. (1995). Distinct coated vesicles labeled for p200 bud from trans-Golgi network membranes. Proc. Natl. Acad. Sci. USA *92*, 2874–2878.

Orci, L., Glick, B.S., and Rothman, J.E. (1986). A new type of coated vesicular carrier that appears not to contain clathrin: its possible role in protein transport within the Golgi stack. Cell *46*, 171–184.

Palade, G. (1975). Intracellular aspects of the process of protein synthesis. Science *189*, 347–358.

Pearse, B.M.F., and Robinson, M.S. (1990). Clathrin, adaptors and sorting. Annu. Rev. Cell Biol. *6*, 151–171.

Pimplikar, S.W., Ikonen, E., and Simons, K. (1994). Basolateral protein transport in streptolysin O-permeabilized MDCK cells. J. Cell Biol. *125*, 1025–1035.

Pimplikar, S.W., and Simons, K. (1993). Regulation of apical transport in epithelial cells by a Gs class of heterotrimeric G protein. Nature *362*, 456–458.

Rabouille, C., Hui, N., Hunte, F., Kieckbusch, R., Berger, E.G., Warren, G., and Nilsson, T. (1995). Mapping the distribution of Golgi enzymes involved in the construction of complex oligosaccharides. J. Cell Sci. *108*, 1617–1627.

Rodriguez-Boulan, E., and Pendergast, M. (1980). Polarized distribution of viral envelope glycoproteins in the plasma membrane of infected epithelial cells. Cell *20*, 45–54.

Rothman, J.E. (1994). Mechanisms of intracellular protein transport. Nature *372*, 55–63.

Rothman, J.E., and Orci, L. (1992). Molecular dissection of the secretory pathway. Nature *355*, 409–415.

Saucan, L., and Palade, G.E. (1994). Membrane and secretory proteins are transported from the Golgi complex to the sinusoidal plasmalemma of hepatocytes by distinct vesicular carriers. J. Cell Biol. *125*, 733–741.

Wagner, M., Rajasekaran, A.K., Hanzel, D.K., Mayor, S., and Rodriguez-Boulan, E. (1994). Brefeldin A causes structural and functional alterations of the trans-Golgi network of MDCK cells. J. Cell Sci. *107*, 933–943.

Wandinger-Ness, A., Bennett, M.K., Antony, C., and Simons, K. (1990). Distinct transport vesicles mediate the delivery of plasma membrane proteins to the apical and basolateral domains of MDCK cells. J. Cell Biol. *111*, 987-1000.

Whitney, J.A., Gomez, M., Sheff, D., Kreis, T.E., and Mellman, I. (1995). Cytoplasmic coat proteins involved in endosome function. Cell *83*, 703–713.

Zacchetti, D., Peranen, J., Murata, M., Fiedler, K., and Simons, K. (1995). VIP17/MAL, a proteolipid in apical transport vesicles. FEBS Lett. *377*, 465–469.